

CHARACTERIZATION OF A BINARY ALKALI-ACTIVATED SYSTEM BASED ON CERAMIC WASTE AND METAKAOLIN

CARACTERIZAÇÃO DO SISTEMA BINÁRIO DE RESÍDUO CERÂMICO E METACAULIM ÁLCALI-ATIVADO

CARACTERIZACIÓN DEL SISTEMA BINARIO DE RESIDUO CERÁMICO Y METACAOLÍN ALCALI- ACTIVADO

JOÃO VICTOR TELES TAVARES | UFC – Universidade Federal do Ceará, Brasil

NAYRA ROCHA DE SOUSA | UFC – Universidade Federal do Ceará, Brasil

ANTONIO LUCAS BRAGA MOREIRA | UFC – Universidade Federal do Ceará, Brasil

ANTONIO EDUARDO BEZERRA CABRAL, Dr. | UFC – Universidade Federal do Ceará, Brasil

HELOINA NOGUEIRA DA COSTA, Dra. | UFC – Universidade Federal do Ceará, Brasil

ABSTRACT

The red ceramic industry generates a substantial amount of solid waste, which can be reutilized in the construction sector, contributing to the reduction of natural resource consumption and CO₂ emissions from the Portland cement industry. However, the use of red ceramic waste as a precursor for alkali-activated materials remains insufficiently investigated. This study aimed to evaluate a binary mixture of red ceramic waste (RCW) and metakaolin (MK) for the production of alkali-activated cements. Four pastes with varying RCW and MK proportions were prepared. In the fresh state, mini-slump, setting time and bulk density tests were performed. In the hardened state, compressive strength was assessed at 7, 28, and 91 days, and water absorption was measured. Finally, scanning electron microscopy (SEM) analysis was conducted. The paste with 100% RCW exhibited the greatest spread (94.5 mm), while the mixture containing 75% MK and 25% RCW achieved the highest compressive strength, reaching 42.79 MPa at 7 days. SEM analysis revealed the formation of binding gels, indicating effective geopolymerization. These findings confirm the feasibility of producing alkali-activated cements from RCW and MK for cementitious paste applications.

KEYWORDS

Construction; Waste; Paste; Alkali-activated binder.

RESUMO

A indústria da cerâmica vermelha é uma grande geradora de resíduos sólidos, que podem ser reaproveitados na construção civil, reduzindo o consumo de recursos naturais e a emissão de CO₂ pela indústria do cimento Portland. No entanto, a aplicação de resíduos de cerâmica vermelha como precursor de materiais álcali-ativados ainda é pouco explorada. Este estudo tem o objetivo de avaliar a mistura binária de resíduo de cerâmica vermelha (RCV) e metacaulim (MK) para obtenção de cimentos álcali-ativados. Foram produzidas quatro pastas com proporções variadas do RCV e MK. No estado fresco, realizaram-se ensaios de mini-slump, tempo de pega e massa específica. No estado endurecido, analisaram-se a resistência à compressão, nas idades de 7, 28 e 91 dias, e a absorção de água. Por fim, foi feito o ensaio de Microscopia Eletrônica de Varredura (MEV). A pasta com 100% RCV apresentou maior espalhamento de 94,5 mm e a composição com 75% MK e 25% RCV apresentou a maior resistência à compressão, com 42,79 MPa aos 7 dias.



A formação de géis aglomerantes foi observada no MEV. Dessa forma, confirma-se a viabilidade do cimento álcali-ativado com RCV e MK para pastas cimentícias.

PALAVRAS-CHAVE

Construção civil; Resíduo; Pasta; Cimento álcali-ativado.

RESUMEN

La industria de la cerámica roja es una gran generadora de residuos sólidos, los cuales pueden ser reutilizados en la construcción civil, reduciendo el consumo de recursos naturales y la emisión de CO₂ por parte de la industria del cemento Portland. Sin embargo, la aplicación de residuos de cerámica roja como precursor de materiales alcaliactivados aún es poco explorada. Este estudio tiene como objetivo evaluar la mezcla binaria de residuo de cerámica roja (RCR) y metacaolín (MK) para la obtención de cementos alcaliactivados. Se produjeron cuatro pastas con proporciones variables de RCR y MK. En estado fresco, se realizaron ensayos de mini-slump, tiempo de fraguado y masa específica. En estado endurecido, se analizaron la resistencia a la compresión, a las edades de 7, 28 y 91 días, y la absorción de agua. Por último, se realizó el ensayo de Microscopía Electrónica de Barrido (MEB). La pasta con 100% de RCR presentó el mayor esparcimiento, con 94,5 mm, y la composición con 75% de MK y 25% de RCR presentó la mayor resistencia a la compresión, con 42,79 MPa a los 7 días. La formación de geles aglomerantes fue observada en el MEB. De esta forma, se confirma la viabilidad del cemento alcaliactivado con RCR y MK para pastas cementicias.

PALABRAS CLAVE

Construcción civil; Residuo; Pasta; Cemento alcaliactivado.

1. INTRODUCTION

The construction industry increasingly seeks sustainable alternatives due to the high carbon dioxide (CO₂) emissions associated with Portland cement (PC) production. One of the strategies to mitigate these emissions is the reduction of clinker consumption, as clinker is the primary component of PC. The clinker production process involves both the calcination of limestone and the combustion of fossil fuels, which together significantly contribute to CO₂ emissions within the cement industry (Miller, Horvath, and Monteiro, 2016).

The cement industry is responsible for approximately 6% to 7% of the anthropogenic CO₂ emissions released annually into the atmosphere (García-Lodeiro, Palomo, and Fernández-Jiménez, 2015). Additionally, cement production requires the extraction of over 30 billion tons of natural resources each year, as highlighted by Jexembayeva et al. (2020). These factors significantly contribute to environmental degradation, intensifying both the depletion of natural resources and the emission of greenhouse gases.

According to Mohajerani et al. (2019), geopolymers and alkali-activated binders can reduce environmental impacts by lowering CO₂ emissions by up to 80% compared to Portland cement, while maintaining comparable mechanical performance.

One effective way to reduce these environmental impacts is through the use of alkali-activated materials (AAMs). Studies have shown that AAMs can lower greenhouse gas emissions by up to 80% compared to Portland cement (Davidovits, 2002). Depending on the precursors and processing conditions, these materials can exhibit a wide range of properties similar to those of conventional cementitious binders. These properties include high compressive strength, low shrinkage, acid and fire resistance, as well as low thermal conductivity (Duxson et al., 2007), alongside an ecologically sustainable profile.

Metakaolin (MK) is widely recognized as one of the most reactive and consistent precursors for geopolymer synthesis, owing to its high degree of amorphicity and well-defined chemical composition (Provis and Bernal, 2014). Furthermore, its use as a partial cement substitute has been extensively studied because of its pozzolanic activity when processed under appropriate conditions (Sabir et al., 2001).

Alkali-activated cements (AACs), also known as geopolymers, are produced by mixing an aluminosilicate source with an alkaline activator, which typically consists of alkaline hydroxides and/or silicates. The most common activators include sodium silicate (Na₂SiO₃), sodium hydroxide (NaOH), potassium silicate (K₂SiO₃), and potassium hydroxide (KOH) (Poudyal and Adhikari, 2021). Aluminosilicate sources may include industrial by-products such as red ceramic waste (RCW), fly ash from thermal power plants, MK, blast furnace slag, among others.

Red ceramic waste can have a chemical composition similar to that of MK, although this depends on the raw materials used. RCW typically contains silica (SiO₂) ranging from 40% to 80% of the total material. Alumina (Al₂O₃) is another significant component, generally present in amounts between 10% and 40% (Medeiros, 2010). In contrast, MK contains approximately 40% Al₂O₃ and 52% SiO₂, totaling around 92% by mass (Nita, 2006). Despite their similar chemical compositions, RCW exhibits lower reactivity than MK, as reported by Schackow et al. (2015). This lower reactivity is attributed to the amorphous and disordered aluminosilicate structure formed during the sintering process.

According to Neto et al. (2016), the generation of red ceramic waste (RCW) is significant due to fragmentation of parts, the presence of non-conforming products, and variations in the sintering process, among other factors. The accumulation and improper disposal of this waste pose serious environmental concerns. Brazilian ceramic industries lose approximately 3 million blocks annually, resulting in around 7,500 tons of waste generated from losses during the ceramic production process, according to the Brazilian Micro and Small Business Support Service (SEBRAE, 2008). The red ceramics industry is primarily responsible for producing bricks and tiles, which account for approximately 90% of the materials used in masonry and roofing in Brazil (ANICER, 2015). These facts underscore the importance of developing sustainable solutions for reusing the waste generated by this sector.

The incorporation of red ceramic waste (RCW) in the production of alkali-activated materials has emerged as a promising and sustainable strategy to reduce environmental impacts. Its use in combination with metakaolin (MK) has been investigated by Rovnaník et al. (2018), who reported improved workability and modifications in the microstructure, although a decrease in the overall reactivity of the system was noted. Similarly, Sarkar and Dana (2021) demonstrated

that substituting up to 30% of MK with ceramic waste can achieve satisfactory levels of mechanical strength, particularly when the activating solution is properly optimized. More recently, Lemouagna et al. (2023) explored the replacement of 70% to 90% of MK with ceramic tile waste in geopolymer composites, achieving compressive strengths of up to 39.6 MPa.

These studies provide valuable insights into the performance of this binary system in alkali-activated cements (AACs). However, further experimental research is needed, particularly to assess the feasibility of utilizing locally sourced RCW. In this context, the main objective of the present study is to investigate the alkaline activation of binary mixtures composed of ceramic waste and metakaolin, including formulations containing 100% ceramic waste. The focus is on evaluating the development of binder properties in paste formulations. To this end, the behavior of the pastes in both fresh and hardened states is analyzed, along with the microstructural characteristics of the resulting materials, to assess the formation of binding phases within the cementitious matrix.

2.1. Materials

2.1.1. Precursors

The RCW, used as an aluminosilicate source, was derived from brick production waste generated by a company located within the Local Productive Arrangement in the state of Ceará, Brazil. The metakaolin was sourced from local suppliers.

The RCW was initially broken manually, then subjected to crushing and milling in a ball mill. After grinding, the material was oven-dried at 105°C for 24 hours and subsequently sieved through a 75µm (No. 200) sieve. Figures 2a and 2b illustrate the visual characteristics of the precursors used.

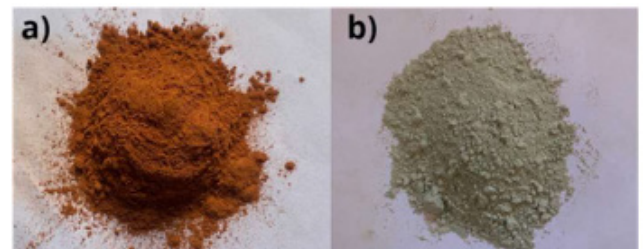


Figure 2: a) Visual aspect of RCW; b) Visual aspect of metakaolin.

Source: The authors, 2025.

2. MATERIALS AND METHODS

Figure 1 summarizes the stages of the experimental program.

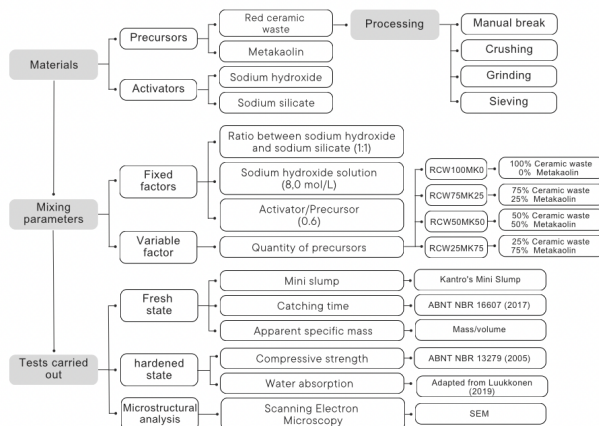


Figure 1: Methodological procedure.

Source: The authors, 2025.

The materials used to make the pastes were: red ceramic waste (RCV), metakaolin (MK), sodium hydroxide (NaOH) and sodium silicate (Na₂SiO₃).

Various tests and analyses were performed to characterize the materials, including laser granulometry, chemical composition, specific gravity, and specific surface area.

Table 1 presents the D10, D50, and D90 values obtained from particle size distribution analysis using laser diffraction, conducted with a Helos KR system (Sympatec).

Features	Diameter (%)	RCW (µm)	MK (µm)
Particle size distribution	D10%	4,60	5,75
	D50%	42,20	31,07
	D90%	89,70	64,89

Table 1: Table Particle size distribution of RCW and MK.

Source: The Authors, 2025.

The chemical composition of the precursors was determined by X-ray fluorescence (XRF) analysis using a Rigaku ZSX Mini II spectrometer. The results for both materials are presented in Table 2.

Components	% de oxides	
	RCW	MK
SiO ₂	58,85	65,44
Al ₂ O ₃	17,82	26,66
Fe ₂ O ₃	6,37	2,87
CaO	2,03	0,70
MgO	1,21	0,39
SO ₃	-	0,19
Na ₂ O	1,70	0,08
K ₂ O	2,27	0,59
TiO ₂	-	1,85
P ₂ O ₅	-	0,07
MnO	-	0,01
Cl	-	0,02
SrO	-	0,04
PF	0,81	0,91

Table 2: Chemical composition of precursors.

Source: The Authors, 2025.

Table 2 indicates that silicon dioxide (SiO₂) and aluminum oxide (Al₂O₃) are the predominant chemical components in both red ceramic waste and metakaolin. A low content of calcium oxide is also present, which is a common constituent in geopolymer precursors.

The specific gravity was determined according to the procedures specified in ABNT NBR 16605 (2017). Additionally, the specific surface area was measured using the Blaine air permeability method, as defined in ABNT NBR 16372 (2015), and compared with a reference cement sample. These characteristics are presented in Table 3.

Characteristic	RCW	MK
Specific gravity	2,65	2,44
Specific surface area (cm ² /g)	2680	10500

Table 3: Physical characteristics of precursors.

Source: The Authors, 2025.

2.1.2. Activators

The alkaline activators used in this study were solid sodium hydroxide (NaOH) with 97.9% purity and a commercial sodium silicate solution. The characterization data for these materials are presented in Table 4.

Parameters	Results
Na ₂ O (%)	15,88
SiO ₂ (%)	32,69
Total Solids (%)	47,77
SiO ₂ (%) / Na ₂ O ratio (silica modulus)	2,17
Specific gravity	1,57
Viscosity (cp)	1,074

Table 4: Characteristics of sodium silicate.

Source: Manufacturer Gota Química (2025).

The alkaline activation solutions were prepared 24 hours before paste formulation. The NaOH solution was prepared at a concentration of 8.0 mol/L (Table 5).

Parameters	8,0 moles/liter
Total Solids – NaOH (%)	25,24
H ₂ O (%)	74,75
H ₂ O / NaOH ratio	2,96
Specific gravity	1,305

Table 5: Characteristics of sodium hydroxide.

Source: The Authors, 2025.

2.2. Research method

2.2.1. Preparation of the paste

Four pastes were prepared with varying proportions of precursors, designated as RCW100MK0 (100% red ceramic waste and 0% metakaolin), RCW75MK25 (75% red ceramic waste and 25% metakaolin), RCW50MK50 (50% red ceramic waste and 50% metakaolin), and RCW25MK75 (25% red ceramic waste and 75% metakaolin). The activator-to-binder ratio was fixed at 0.6, the silicate-to-hydroxide ratio was maintained at 1:1, and the sodium hydroxide solution molarity was set at 8 mol/L. Table 6 details the quantities of materials used to prepare each paste.

Pastes	RCW	MK	NaOH	Na ₂ SiO ₃
RCW100MK0	1557,3	0,0	467,2	467,2
RCW75MK25	1168,0	389,3	467,2	467,2
RCW50MK50	778,6	778,6	467,2	467,2
RCW25MK75	389,3	1168,0	467,2	467,2

Table 6: Quantity of materials in kg/m³.

Source: The Authors, 2025.

Mixing was carried out in a planetary mixer, where the red ceramic waste and metakaolin were combined with the alkaline activators. Initially, the precursors and activators were manually pre-homogenized using a spatula for 60 seconds. The mixture was then placed in the mixer and blended at low speed (62 ± 5 rpm) for 1 minute and 30 seconds. After this, a 60-second pause was observed to assess homogenization. Mixing was resumed for an additional 1 minute and 30 seconds, resulting in a total mixing time of 5 minutes.

2.2.2. Tests Conducted

2.2.2.1. Fresh state

In the fresh state, the workability and fluidity of the paste were evaluated using the mini-slump test (Kantro, 1980).

Setting time was measured according to ABNT NBR 16607 (2017) using a Vicat apparatus. Although this standard was originally developed for Portland cement, it was adapted here for use with alkali-activated cements.

Additionally, in the fresh state, the bulk density was calculated. The volume of the paste was determined using a cylindrical container of known volume. The relationship between mass and volume is expressed by Equation 1.

$$\rho_{um} = \frac{m_s}{V} \quad (1)$$

Where ρ_{um} = bulk density (g/cm^3), m_s = dry mass of the sample (g), V = total volume (cm^3).

Cubic specimens measuring $40 \text{ mm} \times 40 \text{ mm} \times 40 \text{ mm}$ were molded and cured in an oven at 60°C for 24 hours to accelerate geopolymerization. A total of 48 specimens were produced, with 12 cubes corresponding to each paste composition. Demolding was performed 24 hours after casting.

2.2.2.2. Hardened state

To determine compressive strength, three specimens were tested at each curing age, 7, 28, and 91 days, in accordance with ABNT NBR 13279 (2005), as illustrated in Figures 3a and 3b.

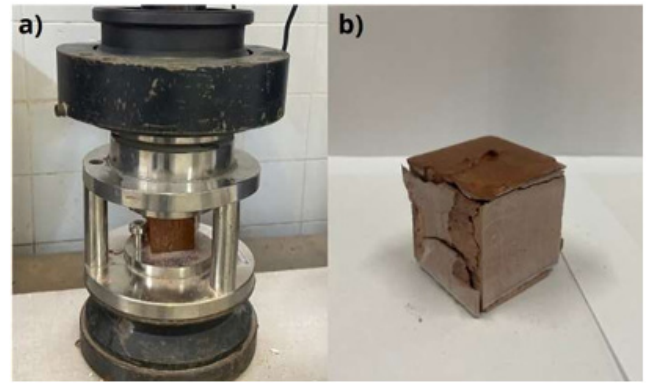


Figure 3: a) axial compressive strength; b) broken specimen.

Source: The authors, 2025.

The water absorption test was adapted from Luukkonen (2019). Specimens were dried in an oven at 60°C for three days, after which their sides were waterproofed with synthetic enamel paint, while the base was submerged in a water bath. The mass of each specimen was measured before water exposure and at 60s, 5 min, 10 min, 20 min, 30 min, 60 min, 2 h, 3 h, 4 h, 6 h, 1 d, 2 d, 3 d, 4 d, 5 d, 6 d and 7d after contact with water.

Equation 2 was used to calculate the percentage of water absorption.

$$I = \frac{m_t}{a \times d} \quad (2)$$

Where I = amount of water absorbed (mm), m_t = sample weight (g), a = surface area in contact with water (mm^2) and d = water density (g/mm^3).



Figure 4: Waterproofed test specimens.

Source: The authors, 2025.

Finally, the microstructural analysis of the hardened pastes was carried out using Scanning Electron Microscopy (SEM). The images were taken in surface mode (SE), which allows the morphology of the particles to be observed. The magnification used was 5000x, guaranteeing a precise view of the structural

characteristics. The equipment used was the QUANTA FEG 450 model from the FEI Company.

3. RESULTS AND DISCUSSIONS

3.1. Fluidity and setting time

The paste composed entirely of red ceramic waste (RCW100MK0) exhibited an average spreading diameter of 94.5 mm, exceeding that of the paste containing 75% RCW and 25% MK, which measured 64.5 mm (Figure 5). In contrast, the pastes with compositions of 50% RCW/50% MK and 25% RCW/75% MK exhibited no measurable spreading, as illustrated in Figure 4. The results obtained in the test were organized and processed using the arithmetic mean and standard deviation of the samples.

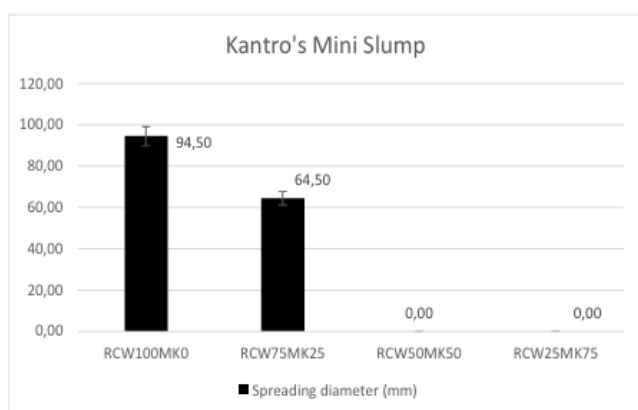


Figure 5: Average spreading diameter in mini slump.

Source: The authors, 2025.

Figure 5 illustrates a decrease in workability as the MK content increases. The pastes RCV50MK50 and RCV75MK25 exhibited the smallest spreading diameters, and further reductions in RCW content resulted in the absence of measurable spreading. This reduced workability is attributed to the high fineness of MK particles, as reported by Pacheco-Torgal et al. (2011) and confirmed here by the Blaine fineness values in Table 3. The high specific surface area of MK increases the demand for the liquid phase, specifically the alkaline activator, which is required to adequately dissolve the particles (Hwang et al., 2019). Conversely, pastes with higher RCW content exhibited greater spreading diameters, supporting the findings of Hwang et al. (2019). The visual appearance and cohesiveness of the pastes are shown in Figure 6.

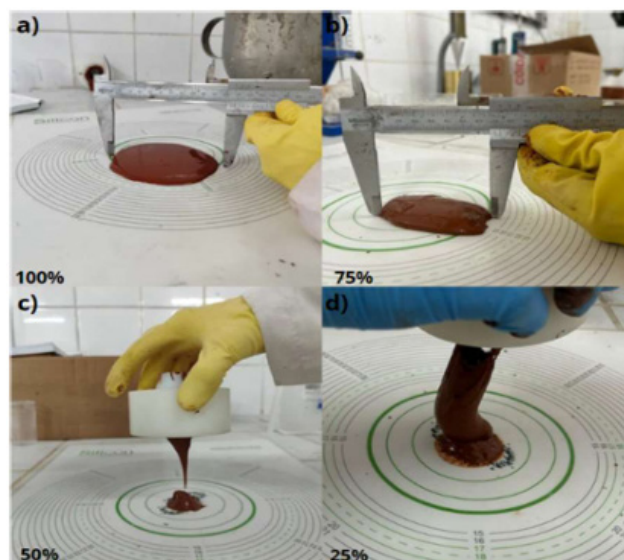


Figure 6: Spreading in the mini slump: a) RCW100MK0; b) RCW75MK25; c) RCW50MK50 e d) RCW25MK75.

Source: The authors, 2025.

Pastes	Bulk density (g/cm ³)
RCW100MK0	2,01
RCW75MK25	1,97
RCW50MK50	1,99
RCW25MK75	1,92

Table 7: Bulk density of the pastes.

Source: The Authors, 2025.

The paste composed exclusively of RCW exhibited the highest bulk density (2.01 g/cm³), indicating a more compact particle structure and lower porosity, consistent with findings reported by Azevedo et al. (2020). As the proportion of MK in the mixtures increased, a corresponding decrease in material density was observed. This trend is attributed to the higher porosity and lower density of MK compared with ceramic waste (Azevedo et al., 2018; Souza, 2020), supporting the data presented in Table 3. The mixture containing 25% RCW and 75% MK showed the lowest density (1.92 g/cm³), which can be explained by the predominance of MK. These results confirm that metakaolin's greater porosity and lower density directly influence the physical properties of the mixtures (Sarkar and Dana, 2021).

The setting time evaluation, shown in Figure 7, revealed that the paste composed of 100% RCW did not harden, remaining unset even after 44 hours. This finding aligns with observations by Hajjaji et al. (2013) and Hwang et al. (2019), who reported that RCW alone lacks sufficient reactivity at room temperature to initiate the formation of a solid matrix.

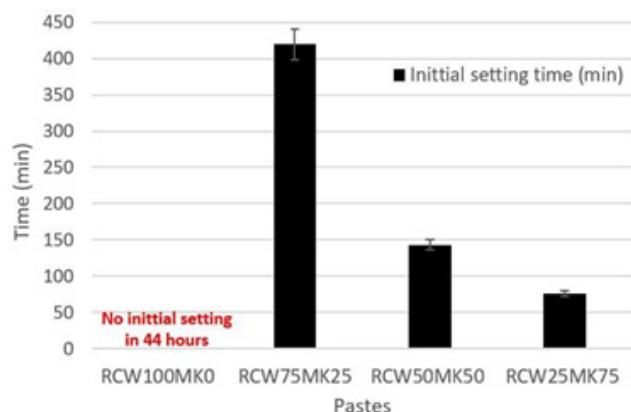


Figure 7: Initial setting time.

Source: The authors, 2025.

In the mixture containing 75% RCW and 25% MK (RCW75MK25), the setting time was 7 hours, a behavior similar to that reported by Souza (2020), who observed prolonged setting times in systems with low MK content. Increasing the MK proportion to 50% reduced the setting time to 2 hours and 23 minutes, indicating an acceleration of the hardening process. This acceleration is attributed to the high reactivity of MK, which promotes the early formation of cementitious products and faster matrix consolidation, as noted by Souza (2003).

When the mixture contained 25% RCW and 75% MK, the setting time was further shortened to 1 hour and 16 minutes, supporting findings by Murta (2015) and Souza (2020), who reported that higher MK content leads to faster setting. These studies confirm that MK accelerates hardening and enhances the reactivity of mixtures, especially in systems initially dominated by less reactive ceramic waste.

The $\text{SiO}_2/\text{Al}_2\text{O}_3$ molar ratio plays a direct role in the setting time of geopolymer pastes. In this study, mixtures with higher MK content exhibited a $\text{SiO}_2/\text{Al}_2\text{O}_3$ ratio of 2.45 and shorter setting times, whereas those with higher RCW content showed a ratio of 3.3 and longer setting times, as illustrated in Figure 7.

As highlighted by Trochez et al. (2015), this behavior is associated with an excess of silicate in the system, which reduces the availability of alumina, thereby slowing the polymerization process and extending the time required for geopolymer matrix consolidation. These findings align with previous research indicating that lower $\text{SiO}_2/\text{Al}_2\text{O}_3$ ratios, with higher Al_2O_3 content, tend to accelerate polymer bond formation and reduce setting time (De Silva et al., 2007; Fletcher et al., 2005).

3.2. Compressive strength and water absorption

The results were reported as the arithmetic mean. Figure 8 shows the average compressive strength at 7, 28, and 91 days.

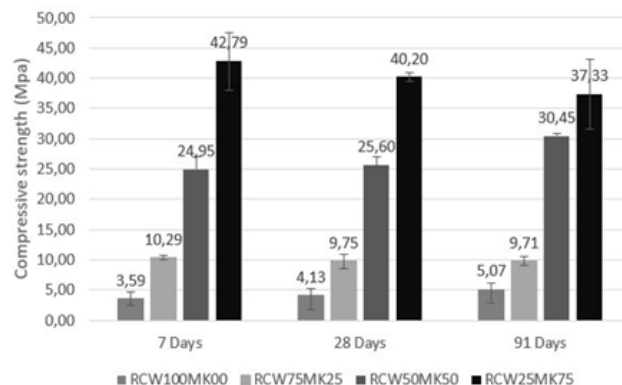


Figure 8: Average axial compressive strength (MPa) - 7, 28, and 91 days.

Source: The authors, 2025.

The progressive replacement of RCW with MK positively influenced the compressive strengths of the samples, as shown in Figure 8, corroborating the findings of Burciaga-Díaz et al. (2016). Similarly, Sarkar and Dana (2021) reported a decrease in compressive strength when MK was partially replaced by RCW in binary mixtures.

The paste composed of 100% RCW exhibited the lowest compressive strength at all tested ages. Pastes containing more than 50% MK demonstrated the highest strengths, consistent with results reported by Kaya and Soyer-Uzun (2016). The RCW50MK50 paste showed an approximate 84% increase in compressive strength compared to the 100% RCW paste (RCW100MK00). The RCW75MK25 paste displayed intermediate performance between RCW100MK00 and RCW50MK50.

The RCW25MK75 paste, with the highest average compressive strength of 40.11 MPa, aligns with Sarkar and Dana's (2021) findings that strength is optimized at around 66% MK content. This enhanced performance is primarily attributed to MK's higher fineness, which provides a larger surface area for chemical reactions.

Additionally, the high content of amorphous phases in MK facilitates its activation and results in greater reactivity compared to RCW, which tends to have a more crystalline structure, as discussed by Zhang et al. (2021) and Souza (2020). Although RCW is rich in essential oxides for geopolymerization, its low reactivity poses a significant limitation, as noted by Alhawati et al. (2024). This limitation is due to the semi-crystalline or

crystalline nature of RCW, which hinders its complete dissolution during alkaline activation.

Souza (2020) emphasizes that this low reactivity compromises the efficient formation of geopolymer gel, negatively affecting the mechanical strength of the pastes. Therefore, the limited dissolution and reactivity of RCW restrict its effectiveness as a geopolymer precursor.

In contrast, mixtures containing 75% MK achieved the highest mechanical performance, reaching compressive strengths of up to 42.79 MPa after 7 days.

For the paste composed entirely of RCW (RCW100MK00), proper hardening did not occur. During demolding at 24 hours, the sample deformed, indicating that the matrix had not developed sufficient rigidity to retain its shape. This behavior, previously reported by Souza (2020), is attributed to the low reactivity of RCW when used alone, which results in inadequate alkaline activation. The absence of a solid matrix prevents the formation of cementitious products, compromising the mechanical properties necessary for structural rigidity. This not only hindered proper hardening but was also the primary cause of the low compressive strengths observed.

3.2.2 Water absorption

Figure 9 shows the water absorption values of the hardened mixtures.

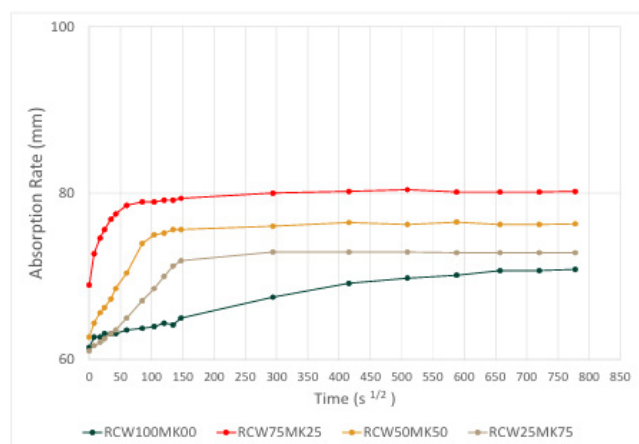


Figure 9: Rate of water absorption over time.

Source: The authors, 2025.

The analysis of water absorption in the alkali-activated pastes revealed distinct behaviors across three time intervals. During the initial period ($t < 60$ s^{1/2}), corresponding to less than one hour, all pastes

exhibited higher absorption rates, particularly those with a greater proportion of RCW. For instance, the RCW75MK25 paste showed a moisture penetration depth of 9.58 mm. This elevated absorption is attributed to the increased connectivity of surface pores. Although the RCW100MK0 paste exhibited a lower initial absorption value (2.08 mm), this measurement does not accurately represent water uptake, as the sample experienced mass loss during the test.

In the intermediate time interval, from 1 hour to 96 hours ($60 \text{ s}^{1/2} < t \leq 587 \text{ s}^{1/2}$), the RCW100MK0 paste demonstrated the highest absorption rate, reaching 6.38 mm, while the other mixtures exhibited a more linear and controlled absorption behavior.

Finally, beyond 96 hours ($t \geq 587 \text{ s}^{1/2}$), absorption rates stabilized across all samples, indicating that the specimens were approaching saturation, with minimal additional water ingress.

The absorption curves presented in Figure 9 underscore the enhanced reactivity of MK and its critical role in pore refinement and void filling within cementitious matrices, resulting in reduced water absorption and improved mechanical strength, consistent with the findings of Zhang et al. (2021). Moreover, Pacheco-Torgal et al. (2011) demonstrated that incorporating MK significantly decreases porosity and enhances the mechanical properties of alkali-activated materials.

The RCW100MK0 samples exhibited anomalous behavior compared to other mixtures, with fragmentation observed during testing, leading to irregular water absorption patterns. This phenomenon is linked to inadequate hardening and insufficient strength development, which undermine the durability and performance of the material, especially under variable load and moisture conditions.

Provis and Bernal (2014) highlight that a stable and consolidated microstructure is essential for preserving the physical and mechanical integrity of alkali-activated materials. The absence of such a microstructure compromises the overall macrostructural properties, adversely affecting durability and service performance.

3.3. Microstructural analysis

Figure 10 presents SEM micrographs illustrating the microstructural characteristics of the binding matrices with varying proportions of RCW and MK.

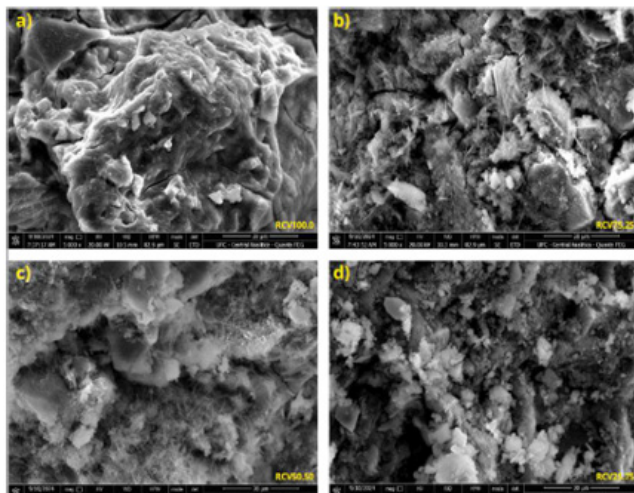


Figure 10: Scanning electron microscopy a) RCW100MK0 b) RCW75MK25 c) RCW50MK50 e d). RCW25MK75.

Source: The authors, 2025.

In the 100% RCW sample (Figure 10a), a highly porous microstructure with prominent cracks and limited formation of cementitious products was observed, characteristic of predominantly crystalline materials with low chemical reactivity. This finding is consistent with Bernal et al. (2014) and Souza (2020), who reported that materials with low reactivity tend to form porous matrices when used as the sole precursor in alkali-activated systems.

With the addition of 25% MK (Figure 10b), the microstructure became notably denser and more compact, accompanied by the initial formation of cementitious gels. Due to the high reactivity of MK, it acted as the primary chemical precursor, reacting with sodium hydroxide and sodium silicate solutions to produce hydrated sodium aluminosilicate (N-A-S-H) gels. These gels serve to bind the RCW particles, partially reducing matrix porosity (Fernández-Jiménez & Palomo, 2005). The filamentous structures observed in the RCW75MK25 and RCW50MK50 samples likely correspond to secondary reaction products and hydrated N-A-S-H gels, which are characteristic features of geopolymeric matrices (Provis et al., 2015).

In the RCW50MK50 mixture (Figure 10c), a more uniform and compact microstructure was observed, with a significant reduction in crack formation. According to studies by Komnitsas and Zaharaki (2007) and Barbosa and MacKenzie (2003), mixtures with a balanced proportion of industrial waste and metakaolin exhibit enhanced mechanical properties due to the formation of a three-dimensional aluminosilicate network. This network effectively fills voids and improves matrix cohesion.

The sample containing RCW25MK75 displayed the densest and most homogeneous microstructure, attributed to the extensive formation of N-A-S-H gels that efficiently integrate the RCW particles into the geopolymeric framework. When metakaolin interacts with sodium hydroxide, it rapidly releases aluminum and silicon ions, which react with sodium silicate to form a characteristic three-dimensional geopolymeric structure. As a result, porosity is nearly eliminated, and the matrix exhibits high potential for mechanical strength and long-term durability (Provis & Bernal, 2014).

4. CONCLUSION

This study evaluated the performance of alkali-activated binary pastes composed of red ceramic waste (RCW) and metakaolin (MK). Based on the experimental results, the following conclusions can be drawn:

- The paste composed entirely of RCW exhibited the highest spreading diameter (94.5 mm), while mixtures containing more than 50% MK showed no measurable flow. This reduction in workability is attributed to the high fineness of MK, which increases the demand for the alkaline activator.
- RCW, when used as the sole precursor, did not harden. The addition of MK significantly accelerated the setting time and promoted hardening due to its higher chemical reactivity, which facilitates the formation of a solid matrix.
- The mixture with 75% MK achieved the highest average compressive strength (40.11 MPa), underscoring the importance of MK as a reactive aluminosilicate source. Its contribution to optimizing the $\text{SiO}_2/\text{Al}_2\text{O}_3$ molar ratio enhanced microstructural development and mechanical performance in alkali-activated systems.
- Water absorption increased with higher RCW content, which correlates with the observed reduction in compressive strength. This relationship highlights the influence of porosity and microstructural integrity on mechanical properties.
- Higher MK content significantly improved the microstructure of the pastes. At 75% MK, the matrix was denser and more homogeneous, resulting in superior mechanical performance. MK enhanced matrix cohesion through the formation of a continuous aluminosilicate network. However, mixtures containing 25% and 50% RCW also showed satisfactory performance, indicating their potential use in producing construction composites such as mortars and concretes.

These findings support the sustainable use of industrial waste as alternative binders, contributing to circular economy practices within the construction sector.

REFERENCES

- ASSOCIAÇÃO BRASILEIRA DE NORMAS TÉCNICAS. ABNT **NBR 16607:2017** – Cimento Portland – Determinação dos tempos de pega. Rio de Janeiro, 2017.
- ASSOCIAÇÃO BRASILEIRA DE NORMAS TÉCNICAS. ABNT **NBR 16605:2017** – Cimento Portland e outros materiais em pó – Determinação da massa específica. Rio de Janeiro, 2017.
- ASSOCIAÇÃO BRASILEIRA DE NORMAS TÉCNICAS. ABNT **NBR 16372:2015** - Cimento Portland - Determinação da finura - Método de Blaine. Rio de Janeiro, 2015.
- ASSOCIAÇÃO BRASILEIRA DE NORMAS TÉCNICAS. ABNT **NBR 13279:2005** - Cimento Portland - Determinação da resistência à compressão. Rio de Janeiro, 2005.
- ASTM INTERNATIONAL. **ASTM C1585-09** - Standard Test Method for Measurement of Rate of Absorption of Water by Hydraulic-Cement Concretes. West Conshohocken, 2009.
- ALHAWAT, M. et al. A study on the influencing parameters in developing construction and demolition waste-based geopolymer concretes and their sustainability assessment. **Construction and Building Materials**, v. 426, p. 136143, 3 maio 2024. Available at: <https://doi.org/10.1016/j.conbuildmat.2024.136143>.
- ALMEIDA, K. S. DE; SOARES, R. A. L.; MATOS, J. M. E. DE. Efeito de resíduos de gesso e de granito em produtos da indústria de cerâmica vermelha: revisão bibliográfica. **Matéria (Rio de Janeiro)**, v. 25, n. 1, 2020.
- ARAUJO, Lucas Benício Rodrigues. Caracterização de misturas álcali-ativadas à base de cinza volante e escória de aciaria. **Dissertação em desenvolvimento (Mestrado em Engenharia Civil)**, Programa de Pós-Graduação em Engenharia Civil: Estruturas e Construção Civil, Universidade Federal do Ceará, Fortaleza, 2022.
- ASSOCIAÇÃO BRASILEIRA DE CERÂMICA. ABCERAM. **Processo de fabricação**. Setor. São Paulo, 2009. Available at: <https://abceram.org.br/processo-de-fabricacao/>. Accessed on Apr. 05, 2024.
- Azevedo, ARG, Vieira, CMF, Ferreira, WM, Faria, KCP, Pedroti, LG, & Mendes, BC (2020). Potential use of ceramic waste as precursor in the geopolymerization reaction for the production of ceramic roof tiles. **Journal of Building Engineering**, 29. doi:10.1016/j.jobbe.2019.101156.
- A. G. DE S. AZEVEDO, K. STRECKER, C. T. LOMBARDI. **Produção de geopolímeros à base de metacaulim e cerâmica vermelha**. v. 64, n. 371, p. 388–396, 1 set. 2018. . Available at: https://www.scielo.br/j/ce/a/NXBhYRkFNXVwqZsFjJMshnP/?utm_source=chatgpt.com. Accessed on Feb. 7, 2025.
- A. GHARZOUNI, E. JOUSSEIN, B. SAMET, S. BAKLOUTI, S. ROSSIGNO. Effect of the reactivity of alkaline solution and metakaolin on geopolymer formation. **Journal of Non-crystalline Solids**, v. 410, p. 127–134, 1 fev. 2015. Available at: <https://doi.org/10.1016/j.jnoncrysol.2014.12.021>.
- BARBOSA, V. F. F.; MACKENZIE, K. J. D. Thermal behaviour of inorganic geopolymers and composites derived from sodium polysialate. **Materials Research Bulletin**, v. 38, n. 2, p. 319–331, 2003.
- BURCIAGA-DÍAZ, O.; GÓMEZ-ZAMORANO, L.Y.; ESCALANTE-GARCÍA, J.I. Influence of the long term curing temperature on the hydration of alkaline binders of blast furnace slag-metakaolin. **Construction and Building Materials**, v. 113, p. 917–926, 1 jun. 2016.
- DAVIDOVITS, J. Environmentally Driven Geopolymer Cement Applications. **Geopolymer 2002 Conference**, 28 out. 2002.
- DUXSON, P.; FERNANDEZ-JIMENEZ, A.; PROVIS, J. L.; LUKEY, G. C.; PALOMO, A.; VAN DEVENTER, J. S. J. Geopolymer technology: The current state of the art. **Journal of Materials Science**, v. 42, n. 9, p. 2917–2933, 2007.
- G.Y. ZHANG, Y.H. AHN, R.S. LIN, X.Y. WANG. Effect of waste ceramic powder on properties of alkali-activated blast furnace slag paste and mortar,

Polymers. **Polymers**, v. 13, n. 16, p. 2817, 22 ago. 2021. Available at: <<https://doi.org/10.3390/polym13162817>>.

GARCÍA-LODEIRO, INES & PALOMO, ANGEL & FERNÁNDEZ-JIMÉNEZ, ANA. An overview of the chemistry of alkali-activated cement-based binders. **Handbook of Alkali-Activated Cements, Mortars and Concretes**, p. 19–47, 1 jan. 2015.

HAJJAJI, W. A., SLÁVKA & CHIARA, ZANELLI & ALSHAAER, MAZEN & DONDI, MICHELE & LABRINCHA, J.A. & ROCHA, F.. (2013). Composition and technological properties of geopolymers based on metakaolin and red mud. **Materials and Design**. 52. 648-654. 10.1016/j.matdes.2013.05.058.

C.L. HWANG, M.D. YEHUALAW, D.H. Vo, T.P. HUYN. Development of high-strength alkali-activated pastes containing high volumes of waste brick and ceramic powders, **Construction and Building Materials**. v. 218, p. 519–529, set. 2019.

JESEMBAYEVA, A., SALEM, T., JIAO, P., HOU, B., & NIYAZBEKOYA, R. Blended Cement Mixed with Basic Oxygen Steelmaking Slag (BOF) as an Alternative Green Building Material. **Materials**, v. 13, n. 14, p. 3062–3062, 9 jul. 2020.

KAYA, Kardelen; SOYER-UZUN, Sezen. Evolution of structural characteristics and compressive strength in red mud–metakaolin based geopolymer systems. **Ceramics International**, v. 42, n. 6, p. 7406-7413, 2016.

KOMNITSAS, K.; ZAHARAKI, D. Geopolymerisation: A review and prospects for the minerals industry. **Minerals Engineering**, v. 20, n. 14, p. 1261-1277, 2007.

LUUKKONEN, T.; HEIKKINEN, J.; KASKELA, A.; LIIRA, H.; HUSGAFVEL, R.; IHALAINEN, M.; LILLINEN, A.; HENRICHSON, C.; KAUKORANTA, P.; NISSINEN, A.; NISSINEN, K. Effect of porosity and pore structure on the performance of geopolymers. **Journal of Materials Science**, Dordrecht: Springer, v. 54, n. 12, p. 10925–10935, 2019. DOI: 10.1007/s10853-019-03641-3.

MARTINS, J. G.; SILVA, A. P. Da. Produtos Cerâmicos. **Série Materiais de Construção**. 2ª edição: UFP, 2004.

MEDEIROS, Leonardo Coutinho de. Adição de cascalho de perfuração da Bacia Potiguar em argilas para uso em materiais cerâmicos: influência da concentração e temperatura de queima. 2010. 101 f. **Dissertação (Mestrado em Ciência e Engenharia de Materiais)** – Universidade Federal do Rio Grande do Norte, Natal, 2010.

MURTA, Frederico Lopes. Produção de argamassas a partir da ativação alcalina de resíduos de cerâmica vermelha e metacaulim. 2015. **Dissertação (Mestrado em Engenharia Civil)** – Universidade Estadual do Norte Fluminense Darcy Ribeiro, Campos dos Goytacazes, 2015. Accessed on Jan. 02, 2025.

MILLER, S. A.; HORVATH, A.; MONTEIRO, P. J. M. Readily Implementable Techniques Can Cut Annual CO2 Emissions from the Production of Concrete by over 20%. **Environmental Research Letters**, v. 11, n. 7, p. 074029, 2016.

MONTEIRO, P. J. M.; MILLER, S. A.; HORVATH, A. Towards sustainable concrete. **Nature Materials**, v. 16, n. 7, p. 698–699, 27 jun. 2017.

DE SILVA, P., SAGOE-CRENSSTIL, K., SIRIVIVATNANON, V., 2007. Kinetics of geopolymerization: Role of Al₂O₃ and SiO₂. **Cement and Concrete Research** **37** (4), 512–518.

FLETCHER, R.A., MACKENZIE, K.J.D., NICHOLSON, C.L., SHIMADA, S., 2005. The composition range of aluminosilicate geopolymers. **Journal of the European Ceramic Society** **25** (9), 1471–1477.

N. MARJANOVIC, M. KOMLJENOVIC, Z. BASCAREVIC, V. NIKOLIC, R. PETROVIC. Physicalmechanical and microstructural properties of alkali-activated fly ash-blast furnace slag blends. **Ceramics International**, v. 41, n. 1, p. 1421–1435, jan. 2015. Available at: <<http://dx.doi.org/10.1016/j.ceramint.2014.09.075>>.

NETO, M. L. Q.; MEDEIROS, M. K. S.; FLORÊNCIO, F. D. C.; JÚNIOR, P. L. S. Geração de resíduo sólido proveniente da fabricação de cerâmica vermelha: caso de indústria cerâmica na região de Assú/RN. 2016.

SILVA, P. D.; SAGOE-CRENSSTIL, K.; SIRIVIVATNANON, V. Kinetics of geopolymerization: Role of Al₂O₃ and SiO₂. **Cement and Concrete Research**, v. 37, n. 4, p. 512–518, abr. 2007.

P. Duxson, S.W. Mallicoat, G.C. Lukey, W.M. Kriven, J.S.J. van Deventer, The effect of alkali and Si/Al ratio on the development of mechanical properties of metakaolin-based geopolymers. **Colloids and Surfaces A: Physicochemical and Engineering Aspects**, v. 292, n. 1, p. 8–20, jan. 2007. Available at: <<https://doi.org/10.1016/j.colsurfa.2006.05.044>>.

PACHECO-TORGAL, F.; MOURA, D.; DING, Y.; JALALI, S. Composition, strength and workability of alkali-activated metakaolin based mortars. **Construction and Building Materials**, v. 25, n. 9, p. 3732–3745, set. 2011. Available at: <<https://doi.org/10.1016/j.conbuildmat.2011.04.017>>.

POUDYAL, L.; ADHIKARI, K. Environmental sustainability in cement industry: An integrated approach for green and economical cement production. **Resources, Environment and Sustainability**, v. 4, p. 100024, mar. 2021.

PROVIS, J. L.; BERNAL, S. A. Geopolymers and Related Alkali-Activated Materials. **Annual Review of Materials Research**, v. 44, n. 1, p. 299–327, jul. 2014.

PROVIS, J. L.; VAN DEVENTER, J. S. J. Alkali Activated Materials: State-of-the-Art Report. **Dordrecht: Springer**, 2015.

SARKAR, MADHUCHHANDA; DANA, KAUSIK. Partial replacement of metakaolin with red ceramic waste in geopolymer. **Ceramics International**, v. 47, n. 3, p. 3473–3483, 2021. ISSN 0272-8842. Available at: <<https://doi.org/10.1016/j.ceramint.2020.09.191>>.

SEBRAE – Serviço Brasileiro de Apoio às Micro e Pequenas Empresas – Cerâmica Vermelha – Estudos de Mercado SEBRAE/ESPM – Relatório Completo. Sebrae Nacional, São Paulo, 2008.

SOUZA, P. S. L. Verificação da influência do uso de metacaulim de alta reatividade nas propriedades mecânicas do concreto de alta resistência. Porto Alegre: Escola de Engenharia da UFRGS, p.203 (**Tese: Doutorado em Engenharia Civil**), 2003.

SOUZA, B. J. L. de. Produção de ligantes geopoliméricos a partir de misturas de resíduos ricos em silicoaluminatos: Resíduo da indústria de cerâmica vermelha, tijolos, telhas e metacaulim. 2020. **Dissertação (Mestrado em Engenharia Civil)**

– Instituto de Tecnologia, Universidade Federal do Pará, Belém, 2020.

TROCHEZ, J.J. et al. Synthesis of geopolymer from spent FCC: Effect of SiO₂/Al₂O₃ and Na₂O/SiO₂ molar ratios. **Materiales de Construcción**. Vol. 65, January–March 2015

W. HUO, Z. ZHU, W. CHEN, J. ZHANG, Z. KANG, S. PU, Y. WAN. Effect of synthesis parameters on the development of unconfined compressive strength of recycled waste concrete powder-based geopolymers. **Construction and Building Materials**. v. 292, p. 123264, 19 jul. 2021. Available at: <<https://doi.org/10.1016/j.conbuildmat.2021.123264>>.

ACKNOWLEDGEMENT

The authors would like to thank Cerâmica Campo Verde Ltda of the Baixo Jaguaribe APL; the National Council for Scientific and Technological Development - CNPq, process no. 409236/2022-5; the Civil Construction Materials Laboratory (LMCC) of the Federal University of Ceará (UFC) - Pici Campus, Fortaleza-CE; the X-ray laboratory of the Physics Department of the Federal University of Ceará - Pici Campus; the Laboratory of Microstructure and Eco-efficiency of Construction Materials (LME) of the University of São Paulo (USP); the Analytical Center of the Federal University of Ceará (UFC).

AUTHORS

ORCID: 0009-0009-7678-8248

JOÃO VICTOR TELES TAVARES | Mestrando em construção civil | Universidade Federal do Ceará – Programa de Pós-Graduação em Engenharia Civil: Estruturas e Construção Civil (PEC) – Campus do Pici. | Fortaleza - CE, Brasil - Cep: 60455-760 | Tel: 85 - 98739-2525
e-mail: joaovictor.engcivil@alu.ufc.br

ORCID: 0009-0004-8209-2240

NAYRA ROCHA DE SOUSA | Graduanda em Engenharia Civil | Universidade Federal do Ceará – Campus Crateús | Endereço: Av. Machadinha Lima, S/N. CEP: 63708-825, Crateús-CE, Brasil | Tel: 88-99972-8148
e-mail: nayrarocha70@gmail.com

ORCID: 0009-0003-5883-2272

ANTONIO LUCAS BRAGA MOREIRA | Graduando em Engenharia

Civil | Universidade Federal do Ceará – Campus Crateús
| Endereço: Av. Machadinho Lima, S/N. CEP: 63708-825,
Crateús - CE, Brasil | Tel: 85-98771-5512
e-mail: moreira.lucass678@gmail.com

ORCID: [0000-0001-6394-1164](https://orcid.org/0000-0001-6394-1164)

ANTONIO EDUARDO BEZERRA CABRAL | Doutor em Ciências da
Engenharia Ambiental | Universidade Federal do Ceará
– Departamento de Engenharia estrutural e construção
civil (DEECC). Campus do Pici, Cep: 60455-760 – Fortaleza-
Ceará– Brasil | Tel: 85-9937-7644
e-mail: eduardo.cabral@ufc.br

ORCID: [0000-0001-9960-2383](https://orcid.org/0000-0001-9960-2383)

HELOINA NOGUEIRA DA COSTA | Doutora em Engenharia e
Ciência de Materiais | Universidade Federal do Ceará –
Campus Crateús | Endereço: Av. Machadinho Lima, S/N.
CEP: 63708-825 | Tel: 85-99147-0802
e-mail: heloina@ufc.br

HOW TO CITE THIS ARTICLE:

TAVARES, J. V. T.; SOUSA, N. R.; MOREIRA, A. L. B.; CABRAL,
A. E. B.; COSTA, H. N. Characterization of a binary
alkali-activated system based on ceramic waste and
metakaolin. **MIX Sustentável**, v.11, n.2, p.109-122. ISSN
2447-3073. Disponível em: <[http://www.nexos.ufsc.br/
index.php/mixsustentavel](http://www.nexos.ufsc.br/index.php/mixsustentavel)>. Acesso em: __/__/__.

SUBMITTED ON: 06/06/2025

ACCEPTED ON: 03/09/2025

PUBLISHED ON: 17/09/2025

RESPONSIBLE EDITORS: Lisiane Ilha Librelotto e Paulo
Cesar Machado Ferroli

Record of authorship contribution:

CRediT Taxonomy (<http://credit.niso.org/>)

JVTT: conceptualization, data curation, formal analysis,
investigation, methodology, resources, visualization
and writing - original draft.

NRS: data curation, formal analysis, resources,
visualization and writing - original draft.

ALBM: data curation, formal analysis, resources,
visualization and writing - original draft.

AEBC: conceptualization, funding acquisition, project
management, validation and and writing - review & editing.

HNC: conceptualization, investigation, methodology,
supervision, validation and and writing - review & editing.

Conflict declaration: nothing to declare.